Quaternary International 433 (2017) 379–392

Contents lists available at ScienceDirect

Quaternary International

journal homepage: www.elsevier.com/locate/quaint

Palaeogeographical reconstruction of the Sierra de Atapuerca Pleistocene sites (Burgos, Spain)

Alfonso Benito-Calvo [a, b, *], Ana Isabel Ortega [a, b], Alfredo Pérez-González [a], Isidoro Campaña [a], José María Bermúdez de Castro [a, c], Eudald Carbonell [d, e]

[a] Centro Nacional de Investigación sobre la Evolución Humana (CENIEH), Paseo de la Sierra de Atapuerca 3, 09002 Burgos, Spain
[b] Grupo Espeleológico Edelweiss, Paseo del Espolón s/n, 09071 Burgos, Spain
[c] UCL Anthropology, 14 Taviton Street, London WC1H 0BW, UK
[d] IPHES, Institut Català de Paleoecología Humana i Evolució Social, C/ Marcelli Domingo s/n Campus Sescelades URV (Edifici W3), 43007 Tarragona, Spain
[e] Universitat Rovira i Virgili (URV), Campus Catalunya, Avinguda de Catalunya 35, 43002 Tarragona, Spain

ARTICLE INFO

Article history:
Available online 13 January 2016

Keywords:
Palaeogeography
Valley evolution
Knickpoint
Paleoanthropological sites
Early–Middle Pleistocene
Sierra de Atapuerca

ABSTRACT

The Sierra de Atapuerca is an anticlinal ridge of Mesozoic carbonate rocks on the NW edge of the Iberian Chain (Northern Spain, Burgos), surrounded by subhorizontal continental sediments of the NE Duero Cenozoic Basin under endorheic conditions. The shift to exorheic conditions in the Duero Basin lead to the onset of an episodic downcutting phase and the development of the Atapuerca multilevel cave system, containing several sites from the Early and Middle Pleistocene. In this work, we have reconstructed the Pleistocene palaeogeographical evolution of the SW flank of the Sierra de Atapuerca, where these archaeological sites are located. The study is based on a detailed geomorphological and geological analysis, combined with Global Navigation Satellite System (GNSS) and 3D LiDAR data, and GIS modeling. These techniques have been applied to analyse the small valleys and the interfluve on the SW flank of the SW Sierra de Atapuerca. The results were combined with the regional base levels recorded by fluvial terraces and the chronostratigraphic sequences of the Sierra de Atapuerca sites. These reconstructions have allowed us to model the palaeogeographical evolution in the nearby area of the cave sites during the Early–Middle Pleistocene, coupling the main formation phases of the sites with the local physical landscape changes that occurred outside the caves. Surface processes are defined by incision phases entailing mitigate knickpoint recession and slope retreatment, and local aggradational phases associated with caves opened and captured by fluvial incision. This reconstruction provides the local physical palaeogeographical habitats developed during the Pleistocene hominid occupation of the Sierra de Atapuerca.

1. Introduction

Palaeogeographical studies are essential to understand the settlement and mobility of human groups since they provide valuable information about site formation processes and past physical landscapes (Mirazón, 2010; Schattner, 2010; Lambeck et al., 2011). Palaeogeographical models can be based on the sedimentological interpretation of stratigraphic records (Stanistreet, 2012), the analysis of relict landforms (Bonnet et al., 2001; Leverington et al., 2002; Benito-Calvo et al., 2008), or the modeling of processes (Kooi and Beaumont, 1994; García-Castellanos et al., 2003).

In this paper we carried out the palaeogeographical reconstruction of the SW flank of the Sierra de Atapuerca through landform correlation and modeling, in order to understand the physical palaeohabitats and the landscape processes characterizing this area during the formation of Early-Middle Pleistocene archaeological sites. These sites contain Early to Middle Pleistocene sequences with several human-bearing layers (Parés and Pérez-González, 1999; Carbonell et al., 2008; Arsuaga et al., 2014; Bermúdez de Castro and Martínón-Torres, 2014; Ortega et al., 2014), which are preserved in allochthonous facies (Pérez-González et al., 1999, 2001; Campaña et al., 2015). The latter are associated with cavity entrances belonging to a Pleistocene multilevel endokarst system related to phreatic levels controlled by fluvial incision (Ortega et al., 2013). The regional base levels were modeled in preliminary investigations (Benito-Calvo et al., 2008).

* Corresponding author. Centro Nacional de Investigación sobre la Evolución Humana (CENIEH), Paseo de la Sierra de Atapuerca 3, 09002 Burgos, Spain.
E-mail address: alfonso.benito@cenieh.es (A. Benito-Calvo).

http://dx.doi.org/10.1016/j.quaint.2015.10.034
1040-6182/

In the current work we deal with the palaeogeographical reconstruction of the nearby area of the archaeological sites.

The SW flank of the Sierra de Atapuerca is characterized by small valleys and hillslopes in the intervening interfluves, where the entrances to the cavities containing the sites are located. These landforms have been studied using a Geographical Information Systems (GIS), high resolution spatial datasets (LiDAR, aerial photographs), and Global Navigation Satellite System (GNSS) surveying. During this work, characteristics of knickpoints and convex shapes identified in longitudinal profiles and hillslopes, were interpreted as non-steady states related to past processes (Loget and Van Den Driessche, 2009; Wegmann et al., 2011; Castillo et al., 2012; Tsou et al., 2014). Through this study we reconstruct the palaeogeographical evolution of the area and the physical landscape inhabited by hominins found in the Sierra de Atapuerca sites.

2. Physical landscape framework

2.1. Geological context

The Sierra de Atapuerca (N42°21′05.29″; W3°30′39.20″; WGS84) is situated in the north-east area of the Duero Depression (north-central Iberian Peninsula), and belongs to the NW part of the Iberian Chain (Fig. 1). In this area, the Sierra de Atapuerca is a gentle anticlinal ridge (1085 m a.s.l.) surrounded by Cenozoic continental sediments. This anticlinal ridge occurs in the SE part of the Bureba Corridor, which is an intermountain depression connecting the Ebro and Duero basins and bounded by the Cantabrian and the Iberian ranges, to the north and south respectively (Fig. 1).

The main geological structure of the Sierra de Atapuerca is described as a NNW–SSE overturned anticline (Pineda and Arce, 1997), faulted and breached in its NW part, where Jurassic and Early Cretaceous rocks crop out (Fig. 2A; Benito-Calvo and Pérez-González, 2015). These rocks are overlain by Late Cretaceous carbonates, mainly consisting of Turonian–Lower Santonian limestones and dolostones (Fig. 2A). Mesozoic formations were folded during the Alpine orogeny, forming the overturned anticline. In the SW limb of this anticline, Late Cretaceous limestones and dolostones show a mean strike of N120°E and dips of 18–20°SW. The main deformation phase occurred during the Oligocene–Lower Miocene, coinciding with the sedimentation of syn-orogenic conglomerates, sandstones and mudstones. During the Neogene, sedimentation of alluvial and lacustrine deposits in Duero Basin took place, represented by several subhorizontal units separated by discontinuities (Armenteros et al., 2002; Alonso-Gavilán et al., 2004). The sequence commences with evaporitic and lacustrine Early Miocene deposits, which are overlain by Middle Miocene alluvial facies topped by a limestone layer (including flint nodules) or a relict palaeosoil. These sediments are overlain by lacustrine sediments of Middle-Late Miocene age, whose carbonates at the top (Lower Páramo limestones) records an phase of major lacustrine expansion. These limestones forms the current top of the Neogene sequence around the Sierra de Atapuerca, although

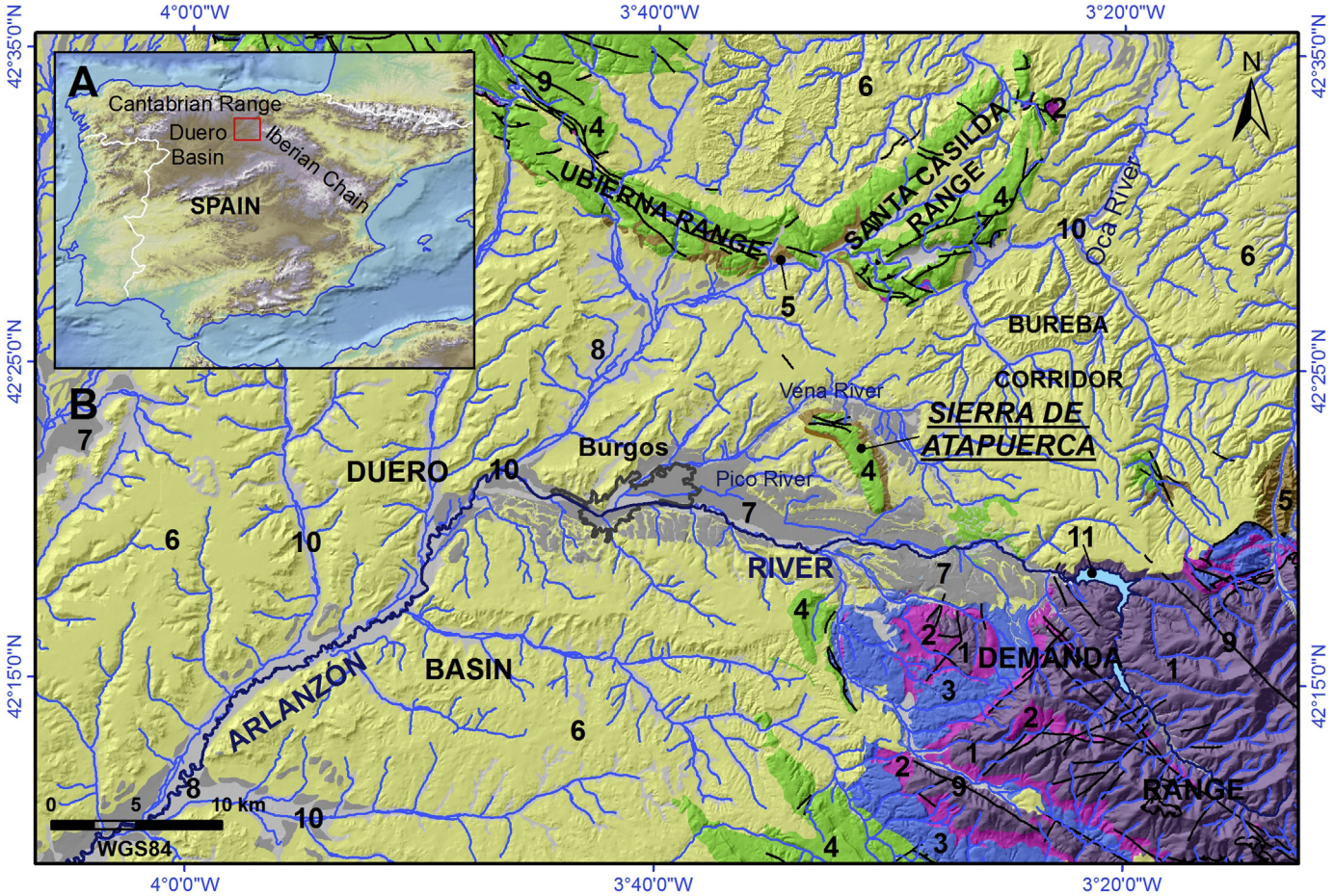

Fig. 1. Study area framework. A) Situation of the NE Duero Basin in the Iberian Peninsula. B) Location of the Sierra de Atapuerca in the NE Duero Basin. Legend: 1, Palaeozoic; 2, Triassic; 3, Jurassic; 4, Cretaceous; 5, Oligocene-Early Miocene; 6, Miocene; 7, Pleistocene; 8, Holocene; 9, Faults; 10, Drainage network; 11, Reservoir.

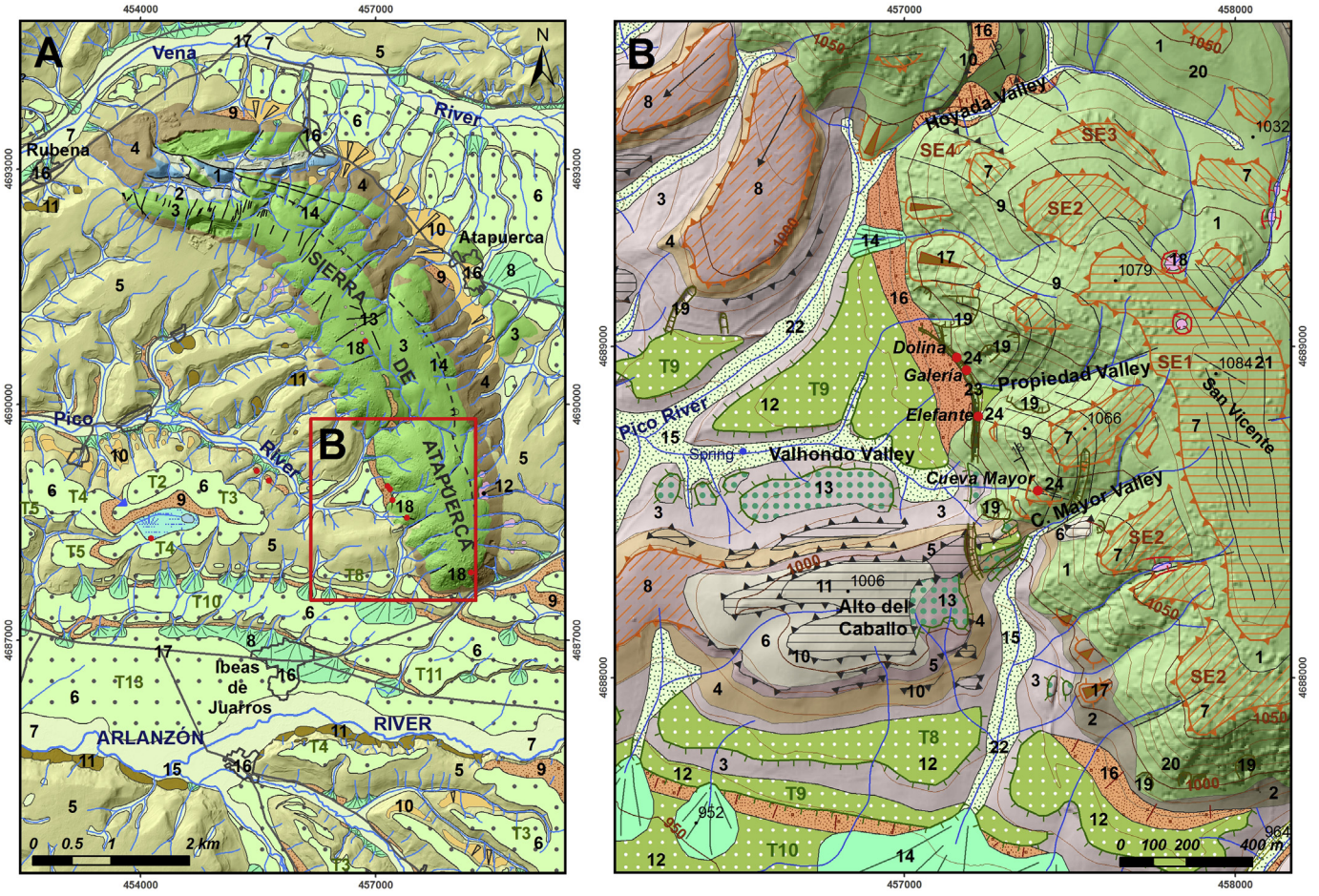

Fig. 2. Geological and geomorphological features in the Sierra de Atapuerca (extracted from Benito-Calvo and Pérez-González, 2015). A) Geological map of the Sierra de Atapuerca (ETRS89). Legend: 1, Limestones (Jurassic); 2, Siliciclastic detrital deposits (Early Cretaceous); 3, Limestones and dolostones (Late Cretaceous); 4, Breccias, conglomerates, sandstones and siltstones (Oligocene–Early Miocene); 5, Alluvial and lacustrine sediments (Miocene); 6, Fluvial terraces (T2–T13); 7, Floodplains and valley beds; 8, Cones; 9, Colluvial deposits; 10, Glacis; 11, Landslides; 12, Dolines; 13, Faults; 14, Anticline; 15, Drainage network; 16, Populations; 17; Roads; 18, Archaeological sites. B) Geomorphological map of the SW flank of the Sierra de Atapuerca (ETRS89). Legend: 1, Limestones and dolostones (Late Cretaceous); 2, Conglomerates and breccias (Oligocene–Early Miocene); 3, Marls and clays (Early Miocene); 4, Clays, marls and sands (Middle Miocene); 5, Limestone layer (Middle Miocene); 6, Marls and limestones, local conglomerates in Cueva Mayor Valley (Late Miocene); 7, Planation surfaces (SE1–SE4); 8, Tilted and exhumated platform (SD2); 9, Rock layers; 10, Structural scarps; 11, Structural platforms; 12, Fluvial terraces (Arlanzón and Pico Valleys), alluvial-colluvial terraces (Cueva Mayor and Propiedad Valleys); 13, Rock terraces; 14, Cones; 15, Valley beds; 16, Colluvial deposits (undifferentiated dumps in Trinchera area); 17, Erosion glacis; 18, Dolines; 19, Quarries and trenches; 20, Contour lines (interval: 10 m); 21, Elevation (m a.s.l.); 22, Drainage network; 23, Trinchera; 24, Archaeological sites (Gran Dolina, Galería, Sima del Elefante, Cueva Mayor).

towards the north and the south a youngest unit crops out, composed of Late Miocene red clays, marls and limestones (García et al., 1997; Benito and Pérez-González, 2005), which represents the youngest sediments of the Duero Neogene Basin. After this endorheic infill (Late Miocene–Pliocene), the Duero Basin was opened to the Atlantic Ocean, giving rise to the development of and incisional fluvial network during the Quaternary.

2.2. Regional geomorphological landforms

The Sierra de Atapuerca and the surrounding areas are characterized by a staircase landscape, comprising stepped planation surfaces, developed during the Neogene endorheic conditions, and fluvial terraces related to the episodic fluvial incision throughout the Quaternary exorheic phase.

In the Sierra de Atapuerca, there are four planation surfaces mainly cut across folded Mesozoic rocks (Zazo et al., 1983; Pérez-González et al., 2001; Benito-Calvo and Pérez-González, 2007). The oldest surface, SE1 (Upper Oligocene–Lower Miocene), truncates the hinge zone of the anticline, forming a plateau at the top of the Sierra de Atapuerca (Fig. 2B). The more recent planation surfaces SE2, SE3 and SE4 were recognized as benches preserved on the anticline limbs (Fig. 2B). SE2 developed during deposition of Middle Miocene alluvial sediments, and ended in the Astaracian due to an uplift event detected in the Sierra de Atapuerca (Benito-Calvo and Pérez-González, 2007), while SE3 is altimetrically related to culminant deposits of the Neogene Duero Basin, during the extensional activity of the Late Miocene. The younger planation surface (SE4) is scarcely preserved on the Sierra de Atapuerca, but is widely represented in the Duero Basin, inset and carved into Late Miocene (Benito-Calvo and Pérez-González, 2015).

During the Quaternary, exorheic fluvial downcutting dissected the planation surfaces. The main fluvial courses of the region are the Arlanzón River, and its tributaries the Vena and Pico rivers (Fig. 2B). In the main fluvial valley, a terrace sequence of 14 levels has been recognized (Zazo et al., 1983; Benito-Calvo et al., 2008, in press), which is composed of terraces with a thin veneer of channel gravel deposits. Chronologies of terrace deposits available in Arnold et al. (2013), Moreno et al. (2012) and Benito-Calvo et al. (2008) are synthesized in Fig. 3. These dates place the terraces between T1

(+92–97 m) and T4 (+60–65 m) in the Early Pleistocene, from T5 (+50–58 m) to T11 (+12–14 m) in the Middle Pleistocene, T12 (+10–11 m) and T13 (+5 m) in the Late Pleistocene, and T14 (+2–3 m) tentatively in the Holocene. The chronologies suggest a significant correlation between terrace deposits and cold Marine Isotope Stages, and have allowed reconstructing the incision rate evolution of the main valley (Benito-Calvo et al., 2015, Fig. 3).

In the Early and Middle Pleistocene, a multilevel endokarst system developed in the Late Cretaceous limestones and dolostones (Ortega Martínez, 2009). The system comprises three levels of subhorizontal water-table controlled galleries with anti-gravitative corrosion features, locally linked by vertical vadose shafts (Ortega et al., 2013, 2014). The subhorizontal galleries appear spatially and chronologically related to some of the Arlanzón fluvial terraces (Ortega et al., 2014, 2013; Benito-Calvo et al., 2015; Parés et al., 2015). The upper level developed in a position similar to the base levels associated with the Lower Páramo limestones, the SE4 planation surface and the fluvial terrace T2 (+82–86 m) (Ortega et al., 2013), which occur at a similar elevation near the Sierra de Atapuerca (Benito-Calvo et al., 2015). The middle and lower cave levels have been correlated to T3 (+70–78 m) and to T4 (+60–65 m)/T5 (+50–54 m) respectively (Ortega Martínez, 2009; Ortega et al., 2013). The karst passages developed during the relative short period of time corresponding to terrace aggradation, while vadose entrenchments are related to prolonged incision phases of the Arlanzón River (Benito-Calvo et al., 2015). During the formation of subhorizontal passages, these galleries were fed from the Arlanzón waters, and emerged at springs in the Pico Valley headwaters (Ortega et al., 2013). Fluvial downcutting progressively changed galleries from phreatic to vadose conditions, starting the allochthonous infilling of the caves through the entrances provided by the old spring areas (Pérez-González et al., 2001, 1999). This processes generated a series of accessible dry caves whose entrances were used by hominids from the Early Pleistocene (Ortega et al., 2014). Currently these cave systems include key hominid-bearing deposits in Europe, such as the Gran Dolina, Galería, Sima del Elefante and Sima de los Huesos (Cueva Mayor) sites (Carbonell et al., 2008; Arsuaga et al., 2014; Bermúdez de Castro and Martínón-Torres, 2014; Ortega et al., 2014).

Landscape evolution in the area is also recorded by landslides, nested piedmonts and colluvial deposits (Benito Calvo, 2004; Benito-Calvo and Pérez-González, 2015). Landslides are mainly concentrated on the scarp carved by the Arlanzón river on the southern valley margin and in structural scarps of Middle Miocene deposits. Nested piedmonts are mainly located in the Vena and Pico Valleys. Colluvial deposits associated with terrace and piedmont scarps include archaeological assemblages belonging to the Late Pleistocene (Hundidero, HC and Fuente Mudarra sites; Navazo, 2006; Navazo et al., 2011; Navazo and Carbonell, 2014; Benito-Calvo et al., 2015).

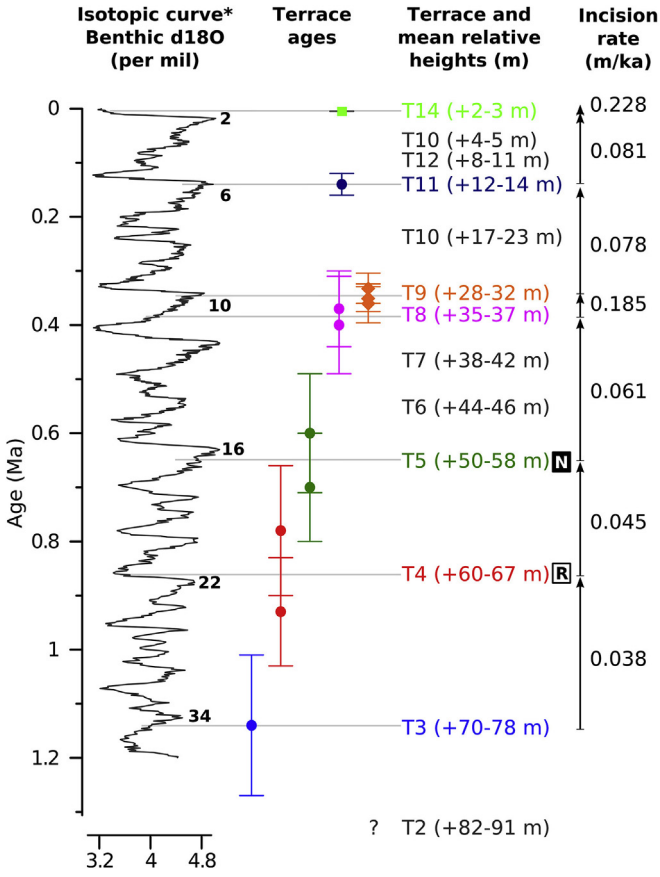

Fig. 3. Sequence of Pleistocene fluvial terraces and incision rates in the Middle Arlanzón Valley, according to Benito-Calvo et al. (2015). Circle shape: ESR dates (Moreno et al., 2012); Diamond shape: TT-OSL dates (Arnold et al., 2013); Square shape: TL dates (Benito-Calvo et al., 2008). Magnetostratigraphic measures: N, normal polarity; R, reversed polarity (Benito-Calvo et al., 2008). *Isotopic curve: Lisiecki and Raymo (2005).

3. Methodology

Palaeogeographical analysis was applied to reconstruct the physical environment of the Pleistocene sites, considering the nearby framework of the SW flank of the Sierra de Atapuerca anticline. These works were based on 1) detailed identification of geomorphological and geological units, 2) correlation and reconstruction of these features considering their relative position and geometrical trends.

Identification of geomorphological and geological units was performed through stereoscopic interpretation of georeferenced digital anaglyphs, produced using aerial photographs of 25 cm resolution (PNOA flight, IGN, Spanish National Geographic Institute), and fieldwork. In general, most landforms and geological deposits were captured using LiDAR DEM data (PNOA, IGN), which has 5 m of resolution and horizontal and vertical accuracies of 1.4 m and 0.5 m respectively. Nevertheless, the SW flank of the Sierra de Atapuerca is partially covered by a dense Mediterranean forest, where LiDAR data does not provide a precise data of the surface topography. In this sector, additional topographic data was collected using a GS15 Leica GNSS system, using Real Time Kinematic (RTK) techniques and the Castilla y Leon GNSS Network, in order to obtain centimetric accuracies. Specifically, GNSS techniques were applied to survey valley and slope topographical profiles, with a mean distance between points of 6 m. These profiles were used to relate local geomorphological features with the location of the archaeological sites and the regional landforms. During this process, convexities in profiles and knickpoints were especially useful. Knickpoints are related to disequilibrium and non-steady states, usually associated with base level lowering, bedrock litho-structural variations, bedload changes or anthropogenic modifications (Burbank and Anderson, 2001; Phillips and Lutz, 2008; Loget and Van Den Driessche, 2009; Castillo et al., 2012). Several estimators can be used to measure curvature and detect convex shapes in profiles (Kerautret et al., 2008). In this work, curvature measures were computed based on deviations from a straight line (Langbein, 1964; Laure, 2008), modified to focus on local variations (Fig. 4). This method estimates curvature, Cv, as the deviation between a point *i* and the straight line joining the points situated before and after the point *i*. Points situated bellow

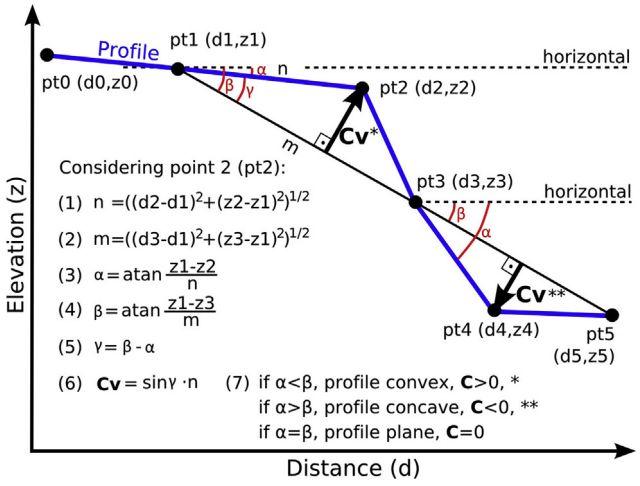

Fig. 4. Method proposed for estimating the curvature (Cv) along the topographic profiles surveyed using centimetric GNSS systems.

the straight line represent concave shapes (negative values), and points situated above the straight line represent convex shapes (positive values). This method was calculated using a spreadsheet, providing an easy and fast way to detect and quantify convexities and concavities in the profiles.

Local geomorphological and geological features around the sites were correlated with regional landforms, in order to reconstruct the landscape palaeogeography. This reconstruction was carried out interpolating the geometrical trends of correlated palaeosurfaces or relit landforms (Bonnet et al., 2001; Leverington et al., 2002; Benito-Calvo et al., 2008; Karampaglidis et al., 2011), by means of statistical methods (polynomial equations and ordinary kriging). Spatial analysis was performed using ArcGIS 10.2.1.

4. Results

Regional base levels in this area were already reconstructed in Benito-Calvo et al. (2008). In this work, we focus on the evolution recorded by the local landforms, which determine the immediate landscape characteristics in the vicinity of the archaeological sites. Local landforms include small valleys and interfluve hillslopes where the cave entrances of the Sierra de Atapuerca sites are located.

4.1. South-west small valleys of the Sierra de Atapuerca

The south-west limb of the Sierra de Atapuerca is drained perpendicularly by small V-shaped valleys, carved from the upper plateau (SE1 planation surface, 1080 m a.s.l.) and in the outcrops of the Neogene sediments, where they converge with the main fluvial courses (Arlanzón River and its tributary, the Pico River). The two small valleys where the known cave entrances are located are Cueva Mayor and Propiedad valleys.

4.1.1. Cueva Mayor Valley

The cave entrance to the Cueva Mayor system is located at the northern margin of the Cueva Mayor Valley, and this valley margin is situated just above the Sima de los Huesos endokarst site. The Cueva Mayor stream is incised into the Late Cretaceous carbonates, and then into Miocene marls and clays (Figs. 2B and 5A). The upper valley incises progressively the planation surfaces SE1–SE3, and contains a local outcrop of a 6 m thick cemented clast-supported conglomerate (Figs. 2B and 5B), which includes interbedded micritic limestones with Miocene ostracoda (Ortega Martínez, 2009). On the other hand, the lower Cueva Mayor stream flows into the Arlanzón valley, forming several alluvial cones on the terrace treads T10 to T13 (Fig. 2A and B), before joining the Arlanzón floodplain at 935 m a.s.l.

In the middle course, near the boundary between the Late Cretaceous carbonates and the Miocene marls, the valley displays a stepped northern margin, which is formed by several tread levels interpreted as terraces (Fig. 2B). The two lower levels correspond to rock-cut terraces developed on Miocene marls and clays, while an upper third level contains colluvial and alluvial deposits (Fig. 5B and C). The latter are composed of matrix-supported breccias with angular clasts to the north, subvertical layers of poorly sorted sands, and clast-supported conglomerates to the south, which reveals a channel morphology with an apparent WSW-ENE strike parallel to the valley (Fig. 5B and D). Between these deposits, a breccia of marls and argillaceous limestones occurs, above a bedrock fracture interpreted by electrical resistivity tomography (Fig. 5B; Ortega et al., 2010). These terraces converge upstream, and are characterized by risers 3–4 m high, which can be recognized in the field along the valley margin until they join with knickpoints preserved on the valley longitudinal profile.

Longitudinal profile knickpoints were detected using curvature and elevation changes (Fig. 5A1 and A2). Knickpoint sections develop in different lithologies and most of them show a distribution independent of significant lithological or structural changes (Fig. 5A1). Knickpoints develops also in soft lithologies, such us marls, clays and unconsolidated Quaternary deposits. Furthermore, knickpoints are geometrically related to geomorphic records of past base level changes (Loget and Van Den Driessche, 2009; Castillo et al., 2012), joining with the risers of the mentioned Cueva Mayor Valley terraces or with planation surface levels (Fig. 5A).

These evidences suggest that knickpoints represent upstream edge of incision waves induces by base level falls (Phillips and Lutz, 2008). On karst terrains, knickpoints stranded and abandoned by subterranean piracy have been described (Fabel et al., 1996), but in Cueva Mayor Valley knickpoints also occur on impermeable marls and clays (Figs. 6 and 7). These characteristics have been used to propose a correlation between the knickpoints, the Cueva Mayor Valley landforms and the Arlanzón fluvial terraces (Fig. 5A). Such correlation allows the reconstruction of the incision evolution of the Cueva Mayor Valley. According to this correlation, Cueva Mayor terraces developed between Arlanzón levels T3 (+82–86 m) and T6 (+44–46 m), and the alluvial-colluvial terrace would be coeval to the formation of the Arlanzón terrace T4 (+60–67 m), whose mean age has been estimated at around 0.85 Ma by means of Electron Spin Resonance (ESR) and reverse palaeomagnetic polarities (Benito-Calvo et al., 2008; Moreno et al., 2012; Benito-Calvo et al., 2015).

4.1.2. Propiedad Valley

Gran Dolina, Sima del Elefante and Galería cavities are located next to the middle Propiedad Valley, just before reaching the outcrops of Neogene sediments. The Upper Propiedad stream follows an E–W direction (Fig. 2B), carved in Late Cretaceous limestones and dolostones (Fig. 6A), and forming a valley incised around 40 m below the planation surface SE2. Then, the valley converges with the Valhondo and Pico Valleys on marl and clay bedrock (Neogene), forming a broad confluence area. Here, the Propiedad stream flows without any significant incision on alluvial-colluvial deposits and on fluvial terrace (Figs. 2B and 6A1). The latter has been dated around 360 ka (Arnold et al., 2013).

Landforms in the Propiedad Valley are mainly restricted to erosion surface SE2 and a Pleistocene alluvial-colluvial infill located in the Trinchera area, just upstream of the contact between the Late

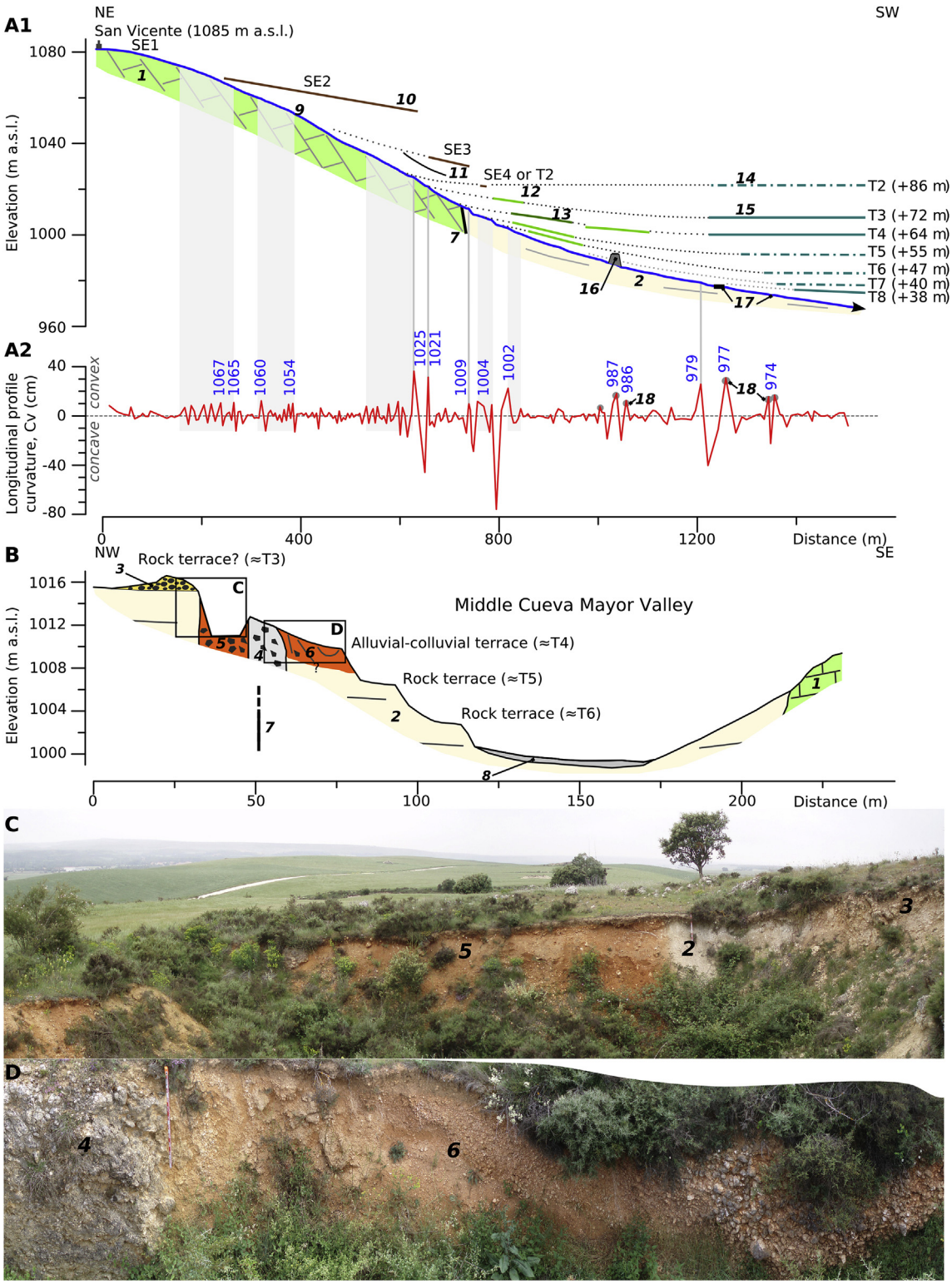

Fig. 5. Cueva Mayor Valley. A1) Cueva Mayor Valley longitudinal profile, geomorphological features and correlation with regional fluvial base levels. A2) Knickpoints identification using longitudinal profile curvature estimation (Fig. 4): blue values represent elevation knickpoint in m a.s.l. B) Perpendicular geomorphological cross-section of the Cueva Mayor Valley. C) and D) Quaternary deposits preserved in the north margin of the Cueva Mayor Valley. Legend: 1, Limestones and dolostones (Late Cretaceous); 2, Clays and marls (Middle and Early Miocene); 3, Conglomerates (Late Miocene); 4, Breccia of marls and argillaceous limestones; 5, Matrix-supported breccia of red mud and limestones (Early Pleistocene?); 6, Mud and sands to the north, and channelised clast-supported conglomerates to the south (Early Pleistocene?); 7, Fault detected by geophysical ETR techniques (Ortega et al., 2010); 8, Bed valley; 9, Cueva Mayor longitudinal profile; 10, Planation surfaces (SE1-SE4); 11, Structural platform on Miocene conglomerates; 12, Rock terraces; 13, Alluvial-colluvial terraces; 14, Base levels of Arlanzón fluvial terraces, reconstructed from downstream and upstream outcrops; 15, Base levels of Arlanzón fluvial terraces preserved on the valley transect; 16, Ballast of old railroad; 17, Tracks; 18, Knickpoints related to anthropogenic modifications (grey circle). (For interpretation of the references to colour in this figure legend, the reader is referred to the web version of this article.)

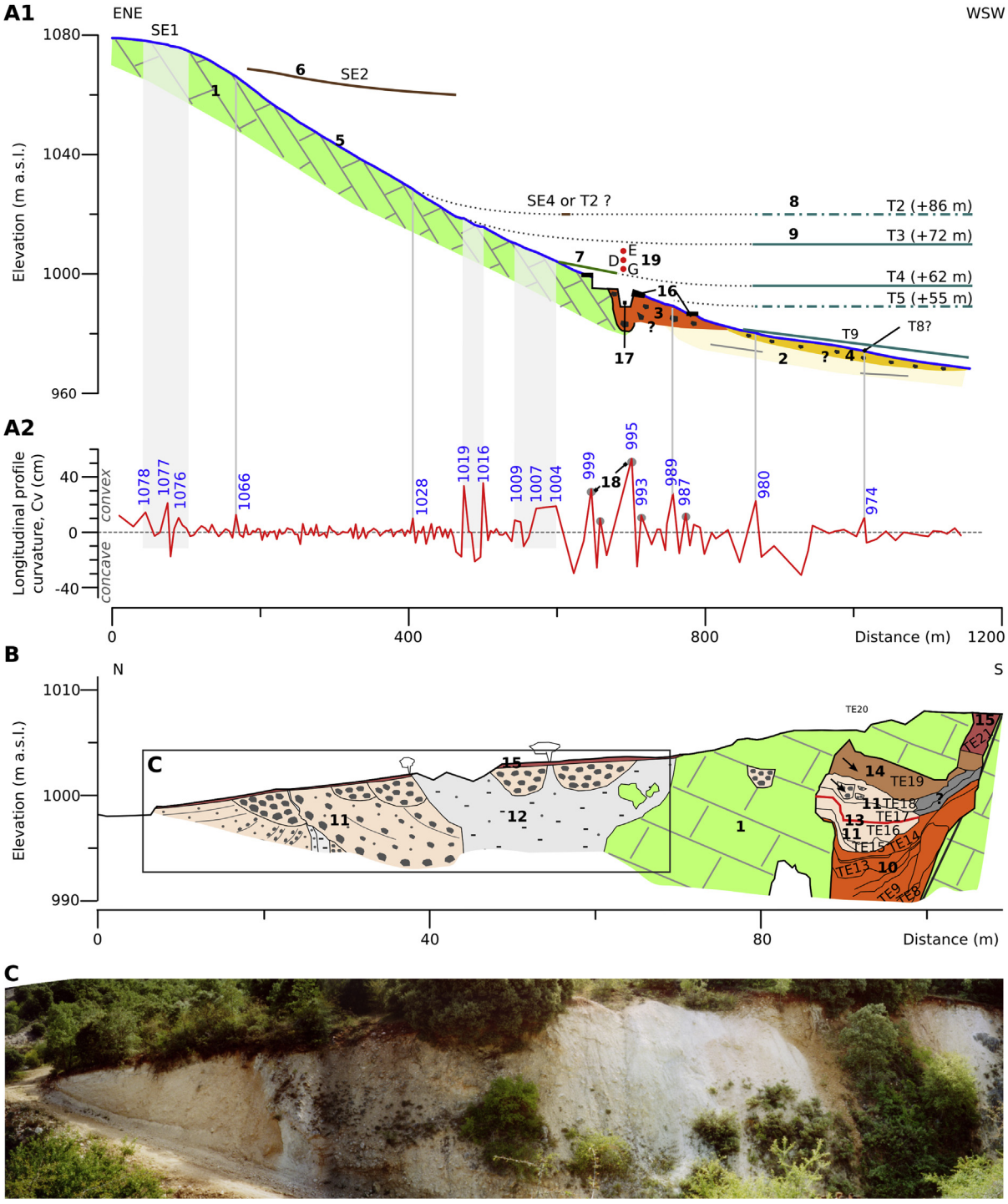

Fig. 6. Propiedad Valley. A1) Propiedad Valley longitudinal profile, geomorphological features and correlation with regional fluvial base levels. A2) Knickpoints identification using longitudinal profile curvatura estimation (Fig. 4): blue values represent elevation knickpoint in m a.s.l. B) Perpendicular geomorphological cross-section of the south margin of the Propiedad Valley. C) Pleistocene infill preserved in the south margin of the Propiedad Valley (modified from Benito Calvo, 2004). Legend: 1, Limestones and dolostones (Late Cretaceous); 2, Clays and marls (Middle and Early Miocene); 3, Alluvial-colluvial valley infill (Early Pleistocene?); 4, Pico Valley fluvial terrace, 0,36 Ma (Arnold et al., 2013); 5, Propiedad Valley longitudinal profile; 6, Planation surfaces (SE1-SE4); 7, Alluvial-colluvial terrace (Early Pleistocene?); 8, Base levels of Arlanzón fluvial terraces, reconstructed from downstream and upstream outcrops; 9, Base levels of Arlanzón fluvial terraces, preserved on the valley transect; 10, Red muds and breccias of the lower Sima del Elefante site unit (Early Pleistocene); 11, Light coloured alluvial sands, muds and conglomerates (Early-Middle Pleistocene); 12, Reworked white marls and clays; 13, Early-Middle Pleistocene boundary in the Sima del Elefante site sedimentary infill (Carbonell et al., 2008); 14, Red-brown breccias (Middle Pleistocene); 15, *Terra rossa* soils; 16, Tracks; 17, Railroad trench and quarries; 18, Knickpoints related to anthropogenic modifications (grey circle); 19, Projected position of the current entrances observed in Trinchera to the sites Sima del Elefante (E), Gran Dolina (D) y Galería (G). Stratigraphical section of Sima del Elefante site modified from Huguet (2007). (For interpretation of the references to colour in this figure legend, the reader is referred to the web version of this article.)

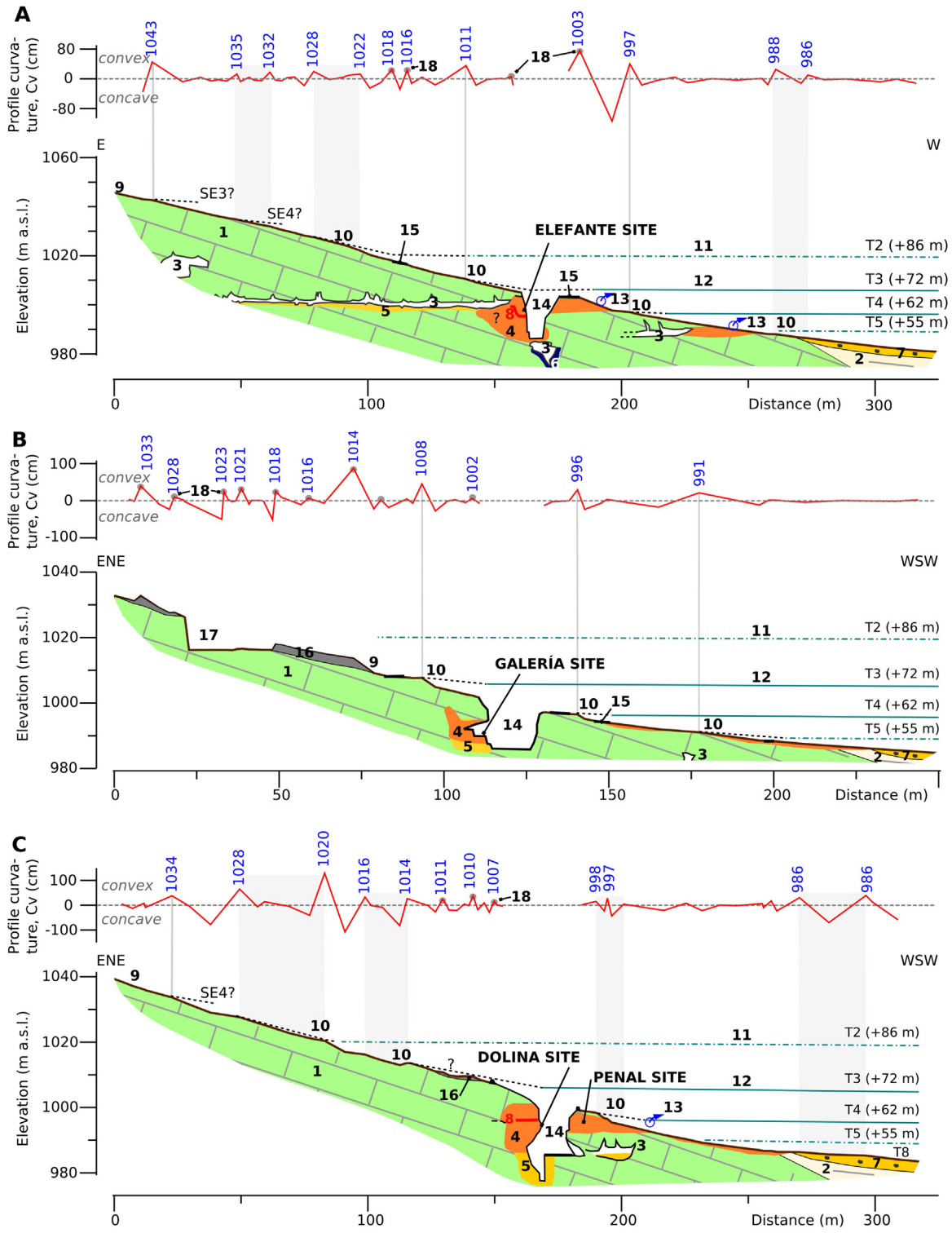

Fig. 7. Slope profiles of the SW flank of the Sierra de Atapuerca. A) Sima del Elefante site profile. B) Galería site profile. C) Gran Dolina site profile. Legend: 1, Limestones and dolostones (Late Cretaceous); 2, Clays and marls (Middle and Early Miocene); 3, Caves, projected on the profile; 4, Alluvial-colluvial deposist; 5, Clays and silts authoctonous facies; 6, Fluvial metamorphic gravels; 7, Pico Valley fluvial terrace, 0.36 Ma (Arnold et al., 2013); 8; Early-Middle Pleistocene boundary; 9, Slope profile; 10, Convex slope breaks identified using elevation and curvature changes (Fig. 4); 11, Base levels of Arlanzón fluvial terraces, reconstructed from downstream and upstream outcrops; 12, Base levels of Arlanzón fluvial terraces, preserved on the valley transect; 13, Pleistocene karstic springs; 14, Railroad trench; 15, Tracks; 16, Dump; 17, Quarries; 18, Knickpoints related to anthropogenic modifications (grey circle).

Cretaceous carbonates and the Miocene mars and clays (Fig. 6A1). Alluvial-colluvial deposits show a minimum exposed thickness of 10 m, and the total has been estimated at 20–24 m by means of electrical resistivity tomography (Ortega et al., 2010). The exposed sequence is composed of several units separated by sharp discontinuities (Benito Calvo, 2004, Fig. 6B and C). Towards the north, the lowest part of the exposed sequence consists mainly of bedded and poorly sorted carbonated sands, and conglomerates filling

palaeochannels. Toward the south, there are white marls and clays, resedimented from Neogene outcrops situated upstream. This white unit is incised by a last unit of conglomerate channels. Similar facies have been detected in caves located in the southern margin of the valley (Fig. 6B), such as conglomerate channels filling small cavities or Sima del Elefante site units. At this site, allochthonous water-laid facies of light coloured sands and conglomerates have been described in units TE15–TE17 coming from Propiedad Valley (Rosas et al., 2006, Fig. 6B). Within this Sima del Elefante site infilling phase, a palaeomagnetic change was detected between units TE16–TE17 (Fig. 6B), associated with the Brunhes–Matuyama reversal change (0.78 Ma, Parés et al., 2006). TE17 has yielded TT-OSL dates between 0.8 and 0.9 Ma for TE16, while TE17 shows probable luminescence ages around 0.72–0.78 Ma (Arnold et al., 2015).

Propiedad Valley infill is currently terraced at 3–4 m above the valley bed, forming a small gently sloping plain, which connects upstream with a valley longitudinal profile knickpoint area preserved on the Late Cretaceous carbonates at 1009–1004 m a.s.l (Fig. 6A1 and A2). On the other hand, the position and trend projection of this plain downstream suggest that is correlative to the regional base level of terrace T4 (+60–68 m), preserved in this transect of the Arlanzón valley at an elevation of 996 m a.s.l. Other knickpoints preserved on the longitudinal profile correlate with Arlanzón terraces T2, T3, T5, and with the Pico fluvial terrace (0.36 Ma, Arnold et al., 2013), equivalent to Arlanzón level T8 (Benito-Calvo and Pérez-González, 2015; Fig. 6A). These correlations also suggest that knickpoint formation along the longitudinal profile was driven by base level changes, and allow the reconstruction of the incision pattern developed by Propiedad Valley during the Early and Middle Pleistocene.

In synthesis, the upper part of these small valleys in the SW flank of the Sierra de Atapuerca contains barely incised Miocene and Early and Middle Pleistocene landforms (erosion surfaces and terraces, Fig. 2), which show upstream convergent longitudinal profiles (Figs. 5 and 6). The geometrical trend of these landforms profiles converge against the current valley longitudinal profiles coinciding with knickpoints sections. Furthermore, in many cases landforms connect directly with knickpoints. These relationships suggest that knickpoints represent the edge of headwater erosion formed during the incision of a base level (Phillips and Lutz, 2008; Loget and Van Den Driessche, 2009; Castillo et al., 2012), being abandoned during the subsequent base level fall in the main valley (Arlanzón valley). During this process, knickpoints can be preferably preserved on resistant lithologies. Nevertheless, in the study area, knickpoints appear distributed independently of lithostructural controls. The abandonment and preservation of these knickpoints are probably due to a low erosional capacity in the headwater area of these small tributaries. This process could be due to subterranean flow piracy related to the Atapuerca endokarst system (Fabel et al., 1996), but knickpoints have been also documented on soft and impermeable clays and marls, and detrital Quaternary sediments. In this way, low erosional capacity during base level falls could be mainly related to the limited drainage area of these small tributary valleys (Foster and Kelsey, 2012), with respect to the main valley. The relationship between knickpoints and base levels also has been observed in other small tributaries located in the Sierra de Atapuerca and the Arlanzón watershed (Benito-Calvo et al., 2008).

4.2. South-west hillslope of the Sierra de Atapuerca

In the study area, gravitational landforms are mainly restricted to landslides and colluvial deposits associated with the Neogene sediments (Fig. 2). Landslides are concentrated at the scarped southern margin of the Arlanzón Valley, and occur with a more disperse pattern on the scarps of Neogene limestones (Fig. 1A). Colluvial deposits are mainly derived from the scarps of depositional landforms (terraces and piedmonts). On the other hand, gravitational landforms in the Sierra de Atapuerca are scarce, being represented by some small colluvial and rockfall areas (Fig. 1B). Slope retreat in the interfluve areas of the Sierra de Atapuerca was already estimated at 0.04–0.27 m/ka, considering the retreat of the slopes from the formation of the planation surfaces SE2 and SE3 until the present day (Benito-Calvo and Pérez-González, 2007; Benito-Calvo et al., 2008).

In this work, we have analysed the slope pattern in the Sierra de Atapuerca SW flank through the study of three GNSS slope profiles passing along the archaeopalaeontological sites of Sima del Elefante, Gran Dolina y Galería. In this area, the Sierra de Atapuerca hillslope is moderately steep (15°), where several slope breaks can be recognized (Fig. 7). Slope morphology is locally affected by human modifications carried out during historic times. Railroad trench (Trinchera), quarries, dumps and tracks have modified the hillside. These modifications are significant in the upper slope of the Galería profile, and to a lesser degree in the Gran Dolina profile (Fig. 7B and C), while in the Sima del Elefante profile they seem less important (Fig. 7A). In the Sima del Elefante profile, several faint convex slope breaks separating hillslope sections and unrelated to anthropogenic alterations were observed at 1022, 1011, 997 and 988 m a.s.l. These slope breaks do not seem to be associated with lithological changes or with significant structures. Although slope breaks are very faint, their position suggests a spatial relationship with fluvial terraces T2–T5, respectively (Fig. 7A). In the Gran Dolina and Galería profiles, a similar correlation pattern could be assumed, considering the areas unaffected by anthropic modifications (Fig. 7B and C). This spatial correspondence could indicate that slope breaks represent phases of retreat in the slopes related to knickpoint propagation and the fluvial incision during the lowering of Pleistocene fluvial base levels (Wegmann et al., 2011; Tsou et al., 2014). Slope failures caused by river incision have also been observed in the main regional valley, the Arlanzón valley (Benito-Calvo and Pérez-González, 2015), and in other main valleys in central areas of the Duero Basin (Yenes et al., 2015).

4.3. Landscape model

Fig. 8 shows the palaeogeographical models proposed for the SW flank of the Sierra de Atapuerca. Palaeolandscape unit maps have been modelled through the geostatistical interpolation of relict landform topography using the ordinary kriging method (Benito-Calvo et al., 2008). The latter was used to recreate the position of the fluvial base level for each period, which determines the incision state of the valleys and the outcropping bedrock units. The models show a gradual hierarchical organization of the fluvial network driven by the Arlanzón River downcutting, whose implications in the SW flank of the Sierra de Atapuerca are explained in the next section.

5. Palaeogeographical evolution of the Sierra de Atapuerca SW flank

The landscape of the Sierra de Atapuerca SW flank shows a complex evolution, as reveal the relict palaeogeographical features that can be traced back to the Neogene. This is not only indicated by the presence of the Neogene deposits and planation surfaces (Fig. 2B; Zazo et al., 1983; Pérez-González et al., 1999; Benito-Calvo and Pérez-González, 2007), but also some characteristics suggest the existence of the Propiedad and Cueva Mayor upper valleys from the Miocene. First, the longitudinal profiles of these valleys display

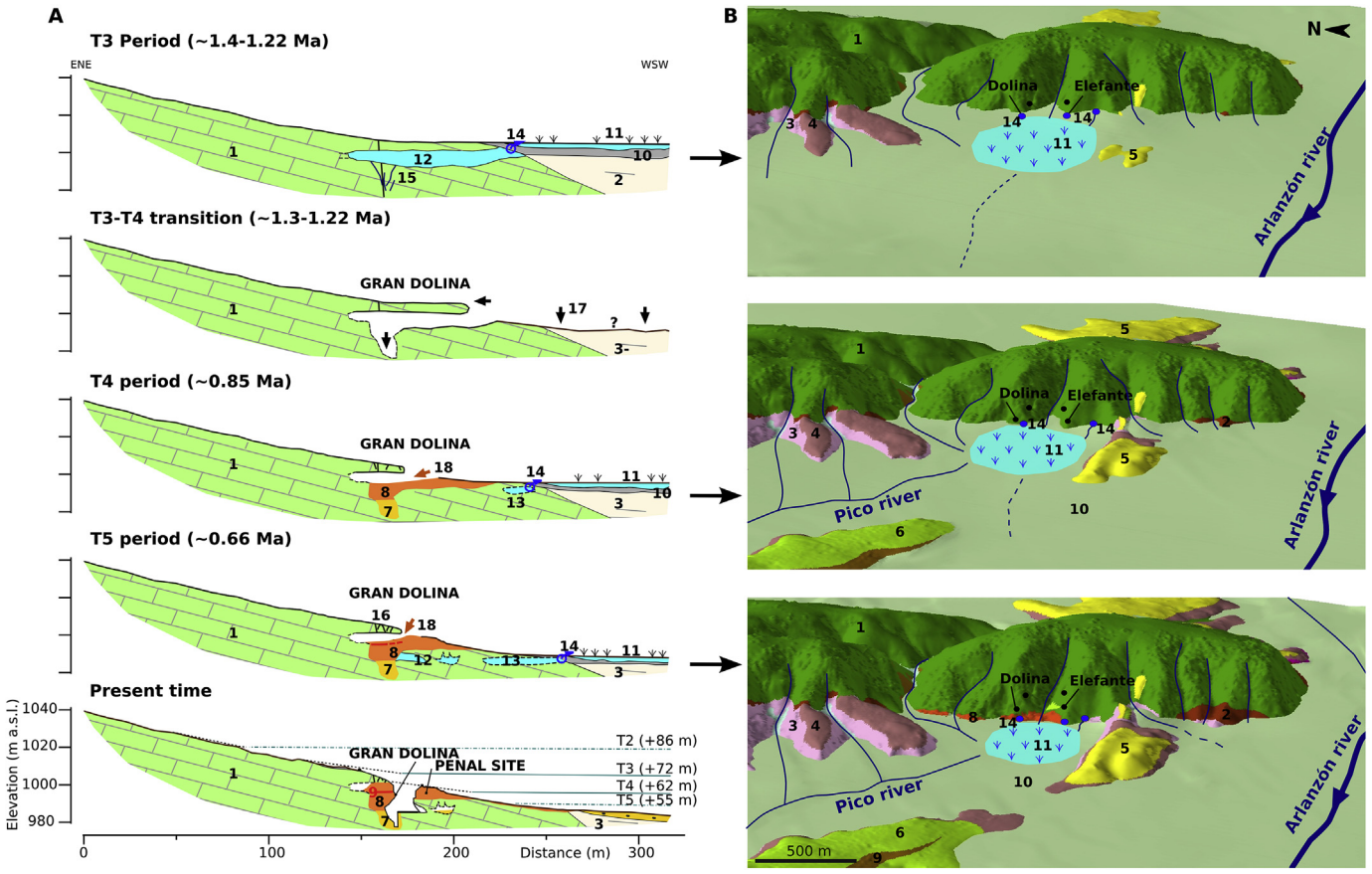

Fig. 8. Palaeogeographical evolution model for the SW flank of the Sierra de Atapuerca during the Early-Middle Pleistocene. A) Hillslope cross-section along Gran Dolina and Penal sites. B) Palaeolandscape units. Legend: 1, Limestones and dolostones, locally flint nodules (Late Cretaceous); 2, Conglomerates (Oligocene-Early Miocene); 3, Marls and clays (Early-Middle Miocene); 4, Limestones with flint nodules (Middle Miocene); 5, Conglomerates, marls and limestones (Upper Miocene); 6, Terraces (Pleistocene); 7, Endogenetic facies (Early Pleistocene): 8, Gravitational and alluvial sediments; 9, Probable colluvial areas; 10, Alluvial floodplain and valley beds; 11; Inferred wetland; 12, Phreatic caves; 13, Phreatic caves, located laterally; 14, Spring areas; 15, Karstification along fractures; 16, Karrens; 17, Incision and slope retreat; 18, Sedimentary inputs.

knickpoints suggesting relict base levels related to the erosion surfaces SE2–SE4 (Figs. 5A and 6A). Besides, these valleys were also filled by Miocene deposits. Propiedad Valley includes Pleistocene white marl and clay reworked deposits (1000–1005 m a.s.l., Fig. 6B and C), which should have come from the erosion of Miocene outcrops situated upstream; and Cueva Mayor Valley even displays an outcrop of Miocene conglomerates (Ortega Martínez, 2009), attached to its margin (Figs. 2B and 8). These conglomerates are located under the uppermost surface of the endorheic Duero Basin (SE3, Benito-Calvo and Pérez-González, 2007; Fig. 5A1 and A2), and their base can be currently observed at 1023 m a.s.l. Such features indicate that the upper rocky valleys, carved around 40 m into Late Cretaceous carbonates, existed with similar current geometries from the Middle–Late Miocene, and were partially filled during the aggradational phases of the Late Miocene endorheic units of the Duero Basin. Later, these Neogene valleys were partially exhumed during the first exorheic phases, in the Plio-Pleistocene (SE4).

From the Plio-Pleistocene boundary to the oldest fluvial terraces recognized in the surroundings (T2, +82–86 m, Fig. 3), local base levels did not change significantly. This caused the persistence of a similar palaeogeography and a relative stable phreatic level (Figs. 6 and 7; Benito-Calvo et al., 2008; Benito-Calvo and Pérez-González, 2015), controlling the formation of the upper endokarst level in the Torcas multilevel cave system of the Sierra de Atapuerca (Ortega et al., 2013). Palaeohydrological evidence found in this endokarst system indicate the presence of karst springs in the SW Sierra de Atapuerca hillslopes (Ortega et al., 2014), which could have fed a probable wetland area in such open valley confluence, located on Miocene impermeable marls and clays (Fig. 8A and B). This probable wetland area could have persisted during the phreatic phase of the endokarst system, associated with the water table levels controlled by terraces T2 (+82–86 m) to T5 (+50–58 m) from the Early to initial Middle Pleistocene (Fig. 3).

During this interval, several processes occurred in the limestone hillslope of the Sierra de Atapuerca, producing significant palaeo-geographical changes in the area of the archaeological sites. Firstly, the period represented for the terrace level T3 (+70–78 m), should predate the formation of the oldest Trinchera sites (Gran Dolina and Sima del Elefante sites, Fig. 8A), since during that period: 1) the local base level in the SW flank for the Sierra de Atapuerca would occupy a higher position than the site entrances (Fig. 6A1 and 7, Benito Calvo, 2004), and 2) the phreatic level of this terrace has been spatially associated with the formation of the intermediate cave level where these sites are located (Ortega et al., 2013). T3 deposition could represent a relative short period of time probably encompassed between 1.13 and 1.22 (Benito-Calvo et al., 2015) or just older than 1.22 (Parés et al., 2015), according to the ages available for the fluvial terrace T3 (1.14 ± 0.13 Ma; Moreno et al., 2012) and for the oldest deposits found in Sima del Elefante site (TE7 and TE9 with 1.13 ± 0.18 and 1.22 ± 0.16 Ma, respectively, Carbonell et al., 2008). All these ages have been described as statistically

undistinguishable (Parés et al., 2015), and are consistent with a Matuyama chronology deduced from reversal palaeomagnetic polarities measured in the endogenetic facies of the intermediate cave level (Parés et al., 2015).

Subsequent to T3 (+70–78 m), Arlanzón River incision reached rates of 0.038 m/ka (Benito-Calvo et al., 2015). In response to this base level drop (T3-T4 transition), the incision of the Pico River began to form a valley separated from the Arlanzón Valley (Fig. 8B). On the other hand, longitudinal profile geometries observed in the Propiedad and Cueva Mayor upper valleys suggest a slow adaptation to this incision (Figs. 6 and 7). The knickpoint recession is incomplete and entails a downstream mean incision rate of only 0.02 m/ka. The latter has been estimated using the vertical incision (6–8 m) which occurred in these upper valleys between terrace T3 and terrace T4. Nevertheless, this general situation shows a certain anomaly in determined areas where these valleys show a significant over-incision. In the Propiedad Valley, a deep incision of >20 m was detected through electrical resistivity tomography (Ortega et al., 2010), probably due to the fluvial incision, capture and opening of previous caves or karstified areas. The valley incision leads also to the vadose vertical entrenchment of the caves belonging to the intermediate cave level, which developed guided by previous limestone fractures (Fig. 8A), as described in Gran Dolina and Sima del Elefante cavities (Ortega et al., 2013). Regarding Cueva Mayor Valley, the incision occurred during the T3–T4 transition is still unknown. However, cavities located under the right margin of this valley (e.g. Cíclopes room) also show phreatic morphologies belonging to the intermediate cave level which suffered a subsequent vadose entrenchment as much as 14 m deep (Ortega et al., 2013). In general, during the peak of this incision phase, the surficial palaeogeography of the SW flank of the Sierra de Atapuerca was characterized by abundant vertical rock cliffs and pits produced by this incision and the vadose karst dissolution.

According to the features observed in the interfluve hillslopes (Fig. 7), the knickpoint propagation during this incision phase also led to a slope retreat phase (Wegmann et al., 2011; Tsou et al., 2014), affecting the areas where the Trinchera sites are currently located. This process eroded the roof of the shallowest and higher cavities (Fig. 8A), leading the backwearing and opening of caves entrances. The latter seems to have occurred first in Sima del Elefante cavity and later in Gran Dolina cavity, according to the chronology of the first allochthonous deposits found in these cavities. The oldest known deposits in Sima del Elefante site are composed of allochthonous facies generated in local open cave conditions between 1.13 ± 0.18 (TE7) and 1.22 ± 0.16 Ma (TE9 human bearing layer, Carbonell et al., 2008); while in Gran Dolina, the oldest sedimentary units consist of >7 m of water-laid facies and speleothems deposited in local close cave conditions (Pérez-González et al., 2001; Campaña et al., 2015), which have been described recently as contemporaneous with the mentioned Sima del Elefante lowest levels (Moreno et al., 2015).

These first sedimentary units could coincide broadly with the transition from incision processes to aggradation processes in the small valleys of the Sierra de Atapuerca. This change should occur in response to the position of the Arlanzón River, although aggradation could have started before and have been faster in these small valleys, due to the anomalous differential relief caused by over-incision geometries. Sedimentary processes in these small valleys led to the accumulation of thick alluvial-colluvial sequences, which contain Neogene reworked deposits, suggesting that Neogene outcrops in the upper small valleys were eroded mainly during this period. As shown in Figs. 5 and 6, the top of the alluvial-colluvial deposits can be correlated spatially with the base level marked by terrace T4 (+60–67 m). This terrace has been dated by mean ages of 0.85 Ma and reversal palaeomagnetic polarities which place it at the end of the Early Pleistocene (Fig. 3; Moreno et al., 2012; Benito-Calvo et al., 2015, 2008). In addition, this age and the altitudinal position of the Propiedad local base level (Fig. 6) coincide with the development of the stratigraphic units TD6 (Gran Dolina site) and TE16 (Sima del Elefante site). Recently, these units have yielded ESR and TT-OSL dates between 0.8 and 0.9 Ma (Arnold et al., 2015; Moreno et al., 2015), and are situated stratigraphically just below the Matuyama-Brunhes reversal detected in both sites (Parés and Pérez-González, 1999; Parés et al., 2006, 2015). Furthermore, the final Early Pleistocene stratigraphic units TE15 and TE16 of the Sima del Elefante site are composed of allochthonous water-laid facies of light coloured sands and conglomerates coming from the Propiedad Valley alluvial-colluvial deposits, indicating that sediments coming from the valley were deposited into the Sima del Elefante cavity during the aggradation phase of the valley. Regarding Gran Dolina, the Early Pleistocene sequence at this site contains perio-dically fluvial facies which could suggest the nearby presence of the local base level (Benito Calvo, 2004; Ortega Martínez, 2009; Campaña et al., 2015). Sedimentation rates characterizing this aggradational period site have been estimated in Gran Dolina at 0.018–0.038 m/ka (Campaña et al., 2015), and at 0.016–0.031 m/ka in the Sima del Elefante, if we consider the ages and thickness available in Carbonell et al. (2008). On the other hand, cavities below the right margin of the Cueva Mayor Valley (Cíclopes room) also show significant aggradation processes represented by inputs of allochthonous breccias, including fluvial sands and silts towards the top (Ortega et al., 2013), with reverse geomagnetic polarities (Parés et al., 2010). Since this cavity was generated during the formation of the intermediate cave level and suffered also the incision processes related to the T3–T4 transition, a plausible correlation for these fluvial deposits could be also the Arlanzón terrace T4.

These inferences allow placing the main formation of the upperpart alluvial-colluvial sequence of the Propiedad and Cueva Mayor valleys at the end of the Early Pleistocene, coinciding with the sedimentation of units TD6 (Gran Dolina), TE16 (Sima del Elefante), the Cíclopes sediments, and during the development of the Arlanzón terrace T4 (+60–67 m). During this period, the vertical topographies generated previously on the SW flank of the Sierra de Atapuerca were partially smoothed, and most of the cavities were partially filled. In addition, the stabilization of the phreatic level during the formation of the Arlanzón terrace T4 led to the formation of the Galería phreatic cavity (Ortega Martínez, 2009). This relationship implies that endogenetic sediments with reversal geomagnetic polarities described in the lower stratigraphic unit of Galería site (GI, Pérez-González et al., 2001, 1999), should have been deposited also at the end of the Early Pleistocene related to the T4 phreatic levels.

Despite this general pattern, the Sima del Elefante sequence also contains Middle Pleistocene allochthonous sediments coming from the Propiedad Valley. These sediments correspond to units TE17 and TE18, which formed at the beginning and during the Middle Pleistocene. TE17 shows normal polarities (Parés et al., 2006; Carbonell et al., 2008) and probable luminiscence ages around 0.78–0.72 (Arnold et al., 2015). The presence of these sediments in the Sima del Elefante TE17 level indicate reworking of the Propiedad Valley deposits, and may be related to the last phase observed in these deposits, recorded by erosional channels (Fig. 6B and C).

The first reworking processes related to TE17 should have occurred during the initial Middle Pleistocene, driven by a new incision phase developed during the T4–T5 transition, which is characterized in the Arlanzón Valley by incision rates of 0.045 m/ky (Benito-Calvo et al., 2015). During this phase, alluvial-colluvial

deposits in the small valleys are terraced, and most of the detected vertical incision occurred in the Miocene bedrock of marls and clays (Figs. 5–7), at rates of 0.03 m/ky. Nevertheless, this base level lowering also drove erosional processes inside the endokarst (Ortega et al., 2013). Later, the aggradation of terrace T5 (+50–58 m) took place at about 0.66 Ma (Fig. 3; Moreno et al., 2012; Benito-Calvo et al., 2015). This date provides a possible final age for the formation of the lower phreatic cave level, which is associated with the water-table level associated with this terrace (Fig. 8; Ortega et al., 2014). This cave level contains quartzite gravels and sands indicanting the entrance of water and sediments from the Arlanzón River, which have been related to T6 (+44–46 m) or higher fluvial events (Ortega et al., 2013). Incision phases occurred in the right margin of the Cueva Mayor Valley after T5 (+50–58 m) could have generated an entrance to Cíclopes or to the Sima de los Huesos (Aranburu et al., 2015).

Subsequently, palaeogeographical changes at the SE flank of the Sierra de Atapuerca mitigated significantly. Due to base level lowering, the endokarst system changed into vadose conditions and springs were deactivated (Ortega et al., 2014). Arlanzón downcutting generated progressively a steeper regional relief (Benito-Calvo et al., 2008), but local terrain roughness on the SW flank of the Sierra de Atapuerca became smoother due to the progressive sealing of cavities. Hillslope processes during Middle Pleistocene were apparently less significant, since sedimentation rates decreased to 0.013–0.016 m/ky in Gran Dolina (Campaña et al., 2015), and to about 0.004 m/ky in Sima del Elefante site, if we consider the thickness between the Bruhness-Matuyama limit (TE16/TE17) and U/Th dates of tufas located to the top of TE18 (254.727 + 13.121/−11.773 ka, and 307.175 + 22.579/−18.868 ka; Bischoff, in de Lombera-Hermida et al., 2015). Discrepancies among the dates available in Galería site (Berger et al., 2008; Falgueres et al., 2013; Demuro et al. 2014) prevent to calculate representative sedimentation rates for the Middle Pleistocene sequence of this site. Open-air, Pico terrace formed around 360 ka in the confluence of Valhondo and Pico Valleys (Arnold et al., 2013). Since then, Cueva Mayor and Propiedad Valleys did not suffer significant evolution, since the lower part of these streams flow on final Middle Pleistocene Arlanzón and Pico terraces without causing vertical incision.

6. Conclusions

GNSS surveying combined with LiDAR data and 25 cm resolution aerial photographs have provided suitable high resolution spatial datasets to recognize and position accurately relict landforms and stratigraphic sequences located around the Early–Middle Pleistocene archaeological sites of the Sierra de Atapuerca. A curvature index was developed to detect convexities shapes in the slope profiles and knickpoints in streams, which were very useful to understand landform evolution in the area. Through these techniques and data we propose a palaeogeographical evolution model, which combines geomorphological and geological features with the site chronostratigraphic sequences. This model reconstructs the processes and physical palaeohabitats characterizing the surface, while a multilevel cave system developed underground.

The landscape is characterised by a moderately steep hillslope on carbonate rocks in SW flank of an anticline incised perpendicularly by small valleys. The latter show several relict landforms and deposits which indicate a slow and incomplete response to base level changes from the Neogene. In the Early–Middle Pleistocene, the cave system probably fed a wetland area downstream. Meanwhile, small valleys formation at the surface occurred through very restricted knickpoint recession and incision, leaving behind local low terraces spatially related to the fluvial terraces of the main regional valley (Arlanzón valley). Valley knickpoint recession seem to cause retreat episodes in the interfluve hillslopes, which would produce the backward migration of the rock roofs and eventualy triggering the new opening of cavities. The slow evolution characterizing the small valleys recorded an anomaly towards the end of the Early Pleistocene, when these valleys incise and capture caves and karstified areas formed previously. This process gives rise to deep incision which developed parallel to the karst vadose entrenchment in the cavities of intermediate karst level, increasing in the area the roughness of the topographic surface. This incision phase is followed by a remarkable aggradation phase which caused the sedimentation of thick alluvial-colluvial sequences in certain areas of the valleys, and the water-laid and gravity flow successions observed in the archaeological sites. This aggradational phase probably finished in the valleys at the end of the Early Pleistocene (0.8–0.9 Ma), coinciding with the stabilization of the regional base level in the Arlanzón fluvial terrace T4 (+60–67 m).

Acknowledgements

This study was supported by research projects CEN001B10–2 (Junta de Castilla y León) and CGL 2012-38434-C03-02 (DGICYT). The authors thank the archaeopalaeontological research team of the Sierra de Atapuerca for constant scientific and logistic support. R. Pérez Martínez surveyed the GNSS topographic profiles along the slope of the Sierra de Atapuerca. We thank O. Magri, F. Gutiérrez and an anonymous reviewer for the useful comments and the detailed revision.

References

Alonso-Gavilán, G., Armenteros, I., Carballeira, J., Corrochano, A., Huerta, P., Rodríguez, J.M., 2004. Cuenca del Duero. In: Vera, J.A. (Ed.), Geología de España. Sociedad Geológica de España. IGME., Madrid, pp. 550–556.

Aranburu, A., Arsuaga, J.L., Sala, N., 2015. The stratigraphy of the Sima de los Huesos (Atapuerca, Spain) and implications for the origin of the fossil hominin accumulation. Quaternary International. http://dx.doi.org/10.1016/j.quaint.2015.02.044.

Armenteros, I., Corrochano, A., Alonso-Gavilán, G., Carballeira, J., Rodríguez, J.M., 2002. Duero Basin (northern Spain). In: Gibbons, W., Moreno, T. (Eds.), Geology of Spain. The Geological Society, London, pp. 309–315.

Arnold, L.J., Demuro, M., Navazo, M., Benito-Calvo, A., Pérez-González, A., 2013. OSL dating of the Middle Palaeolithic Hotel California site, Sierra de Atapuerca, north-central Spain. Boreas 42, 285–305.

Arnold, L.J., Demuro, M., Parés, J.M., Pérez-González, A., Arsuaga, J.L., Bermúdez de Castro, J.M., Carbonell, E., 2015. Evaluating the suitability of extended-range luminescence dating techniques over early and Middle Pleistocene timescales: published datasets and case studies from Atapuerca, Spain. Quaternary International. http://dx.doi.org/10.1016/j.quaint.2014.08.010.

Arsuaga, J.L., Martínez, I., Arnold, L.J., Aranburu, A., Gracia-Téllez, A., Sharp, W.D., Quam, R.M., Falguères, C., Pantoja-Pérez, A., Bischoff, J., Poza-Rey, E., Parés, J.M., Carretero, J.M., Demuro, M., Lorenzo, C., Sala, N., Martinón-Torres, M., García, N., Alcázar De Velasco, A., Cuenca-Bescós, G., Gómez-Olivencia, A., Moreno, D., Pablos, A., Shen, C.-C., Rodríguez, L., Ortega, A.I., García, R., Bonmatí, A., Bermúdez De Castro, J.M., Carbonell, E., 2014. Neandertal roots: cranial and chronological evidence from Sima de los Huesos. Science 344, 1358–1363. http://dx.doi.org/10.1126/science.1253958.

Benito, A., Pérez-González, A., 2005. Las superficies erosivas de los páramos en el sector NE de la Cuenca del Duero y sus implicaciones en la conexión Duero-Bureba. Boletín Geológico y Minero 116, 351–360.

Benito Calvo, A., 2004. Análisis geomorfológico y reconstrucción de paleopaisajes neógenos y cuaternarios en la Sierra de Atapuerca y el valle medio del río Arlanzón. Universidad Complutense de Madrid, Madrid.

Benito-Calvo, A., Ortega, A.I., Navazo, M., Moreno, D., Pérez-Gonzalez, A., Parés, J.M., Bermúdez De Castro, J.M., Carbonell, E., 2015. Pleistocene Geodynamic Evolution of the Arlanzón valley: Implications for the Formation of the Endokarst System and the Open Air Archaeological Sites of the Sierra de Atapuerca (Burgos, España). Boletín Geológico y Minero (in press).

Benito-Calvo, A., Pérez-González, A., 2015. Geomorphology of the Sierra de Atapuerca and the Middle Arlanzón Valley (Burgos, Spain). Journal of Maps 11, 535–544. http://dx.doi.org/10.1080/17445647.2014.909339.

Benito-Calvo, A., Pérez-González, A., 2007. Erosion surfaces and Neogene landscape evolution in the NE Duero Basin (north-central Spain). Geomorphology 88, 226–241. http://dx.doi.org/10.1016/j.geomorph.2006.11.005.

Benito-Calvo, A., Pérez-González, A., Parés, J.M., 2008. Quantitative reconstruction of Late Cenozoic landscapes: a case study in the Sierra de Atapuerca (Burgos,

Spain). Earth Surface Processes and Landforms 33, 196–208. http://dx.doi.org/10.1002/esp.1534.
Berger, G.W., Pérez-González, A., Carbonell, E., Arsuaga, J.L., Bermúdez de Castro, J.-M., Ku, T.-L., 2008. Luminescence chronology of cave sediments at the Atapuerca paleoanthropological site, Spain. Journal of Human Evolution 55, 300–311.
Bermúdez De Castro, J.M., Martinón-Torres, M., 2014. Evolutionary interpretation of the modern human-like facial morphology of the Atapuerca Gran Dolina-TD6 hominins. Anthropological Science 122, 149–155. http://dx.doi.org/10.1537/ase.140827.
Bonnet, S., Bernard, M., Driessche, J.V., 2001. Drainage network expansion of the Salagou drainage basin (S. France): an example of relief response to recent climate change? Terra Nova 13, 214–219.
Burbank, D.W., Anderson, R.S., 2001. Tectonic Geomorphology. Backwell, Oxford.
Campaña, I., Benito-Calvo, A., Pérez-González, A., Ortega, A.I., Bermúdez de Castro, J.M., Carbonell, E., 2015. Pleistocene Sedimentary facies of the Gran Dolina Archaeo-Paleoanthropological Site (Sierra de Atapuerca, Burgos, Spain). http://dx.doi.org/10.1016/j.quaint.2015.04.023.
Carbonell, E., Bermúdez de Castro, J.M., Parés, J.M., Pérez-González, A., Cuenca-Bescos, G., Ollé, A., Mosquera, M., Huguet, R., van der Made, J., Rosas, A., Sala, R., Vallverdú, J., García, N., Granger, D.E., Martinón-Torres, M., Rodríguez, X.P., Stock, G.M., Vergès, J.M., Allué, E., Burjachs, F., Cáceres, I., Canals, A., Benito, A., Díez, C., Lozano, M., Mateos, A., Navazo, M., Rodríguez, J., Rosell, J., Arsuaga, J.L., 2008. The first hominin of Europe. Nature 452, 465–469. http://dx.doi.org/10.1038/nature06815.
Castillo, M., Bishop, P., Jansen, J.D., 2012. Knickpoint retreat and transient bedrock channel morphology triggered by base-level fall in small bedrock river catchments: the case of the Isle of Jura, Scotland. Geomorphology, 180–181, 1–9. http://dx.doi.org/10.1016/j.geomorph.2012.08.023.
de Lombera-Hermida, A., Bargalló, A., Terradillos-Bernal, M., Huguet, R., Vallverdú, J., García-Antón, M.-D., Mosquera, M., Ollé, A., Sala, R., Carbonell, E., Rodríguez-Álvarez, X.-P., 2015. The lithic industry of Sima del Elefante (Atapuerca, Burgos, Spain) in the context of Early and Middle Pleistocene technology in Europe. Journal of Human Evolution 82, 95–106. http://dx.doi.org/10.1016/j.jhevol.2015.03.002.
Demuro, M., Arnold, L.J., Parés, J.M., Pérez-González, A., Ortega, A.I., Arsuaga, J.L., Bermúdez de Castro, J.M., Carbonell, E., 2014. New luminescence ages for the Galería Complex archaeological site: resolving chronological uncertainties on the acheulean record of the Sierra de Atapuerca, Northern Spain. PLoS One 9, e110169. http://dx.doi.org/10.1371/journal.pone.0110169.
Fabel, D., Henricksen, D., Finlayson, B.L., Webb, J.A., 1996. Nickpoint recession in karst terrains: an example from the Buchan Karst, Southeastern Australia. Earth Surface Processes and Landforms 21, 453–466 doi:10.1002/(SICI)1096-9837(199605)21:5<453::AID-ESP608>3.0.CO;2–4.
Falguères, C., Bahain, J.-J., Bischoff, J.L., Pérez-González, A., Ortega, A.I., Ollé, A., Quiles, A., Ghaleb, B., Moreno, D., Dolo, J.-M., Shao, Q., Vallverdú, J., Carbonell, E., Bermúdez de Castro, J.M., Arsuaga, J.L., 2013. Combined ESR/U-series chronology of Acheulian hominid-bearing layers at Trinchera Galería site, Atapuerca, Spain. Journal of Human Evolution 65, 168–184. http://dx.doi.org/10.1016/j.jhevol.2013.05.005.
Foster, M.A., Kelsey, H.M., 2012. Knickpoint and knickzone formation and propagation, South Fork Eel River, northern California. Geosphere 8, 403–416. http://dx.doi.org/10.1130/GES00700.1.
García, A., Cabra, P., Solé, J., 1997. Mapa Geológico de España, E 1:50.000, Hoja n° 238 (Villagonzalo-Pedernales), Serie Magna. IGME, Madrid.
García-Castellanos, D., Vergés, J.M., Gaspar-Escribano, J., Cloetinhg, S., 2003. Interplay between tectonics, climate, and fluvial transport during the Cenozoic evolution of the Ebro Basin (NE Iberia). Journal of Geophysical Research 108, 2347. http://dx.doi.org/10.1029/2002JB002073.
Huguet, R., 2007. Primeras ocupaciones humanas en la Península Ibérica: Paleoeconomía en la Sierra de Atapuerca (Burgos) y la Cuenca de Guadix-Baza (Granada) durante el Pleistoceno Inferior. Universitat Rovira i Virgili, Tarragona.
Karampaglidis, T., Benito Calvo, A., Pérez-González, A., Baquedano, E., Arsuaga, J.L., 2011. Secuencia geomorfológica y reconstrucción del paisaje durante el Cuaternario en el Valle del río Lozoya (Sistema Central, España). Boletín de la Real Sociedad Española de Historia Natural 105, 149–162.
Kerautret, B., Lachaud, J.-O., Naegel, B., 2008. Comparison of Discrete Curvature Estimators and Application to Corner Detection, Lecture Notes in Computer Science (Including Subseries Lecture Notes in Artificial Intelligence and Lecture Notes in Bioinformatics).
Kooi, H., Beaumont, C., 1994. Escarpment evolution on high-elevation rifted margins: insights derived from a surface processes model that combines diffusion, advection, and reaction. Journal of Geophysical Research 99, 12191–12209.
Lambeck, K., Purcell, A., Flemming, N.C., Vita-Finzi, C., Alsharekh, A.M., Bailey, G.N., 2011. Sea level and shoreline reconstructions for the Red Sea: isostatic and tectonic considerations and implications for hominin migration out of Africa. Quaternary Science Reviews 30, 3542–3574.
Langbein, W.B., 1964. Profiles of Rivers of Uniform Discharge. U.S. Geological Survey Professional Paper 501B, pp. 119–122.
Larue, J.-P., 2008. Effects of tectonics and lithology on long profiles of 16 rivers of the southern Central Massif border between the Aude and the Orb (France). Geomorphology 93, 343–367. http://dx.doi.org/10.1016/j.geomorph.2007.03.003.
Leverington, D.W., Teller, J.T., Mann, J.D., 2002. A GIS method for the reconstruction of late Quaternary landscapes from isobase data and modern topography. Computers & Geosciences 28, 631–639.
Lisiecki, L.E., Raymo, M.E., 2005. A Pliocene-Pleistocene stack of 57 globally distributed benthic δ18O records. Paleoceanography 20, 1–17. http://dx.doi.org/10.1029/2004PA001071.
Loget, N., Van Den Driessche, J., 2009. Wave train model for knickpoint migration. Geomorphology 106, 376–382. http://dx.doi.org/10.1016/j.geomorph.2008.10.017.
Mirazón, M., 2010. Saharan corridors and their role in the evolutionary geography of "Out of Africa I,". In: Fleagle, J.G., Shea, J.J., Grine, F.E., Baden, A.L., Leaky, R.E. (Eds.), Out of Africa I: the Frist Hominin Colonization of Eurasia. Springer, London, New York, pp. 27–46.
Moreno, D., Falguères, C., Pérez-González, A., Duval, M., Voinchet, P., Benito-Calvo, A., Ortega, A.I., Bahain, J.J., Sala, R., Carbonell, E., Bermúdez de Castro, J.M., Arsuaga, J.L., 2012. ESR chronology of alluvial deposits in the Arlanzón valley (Atapuerca, Spain): contemporaneity with Atapuerca Gran Dolina site. Quaternary Geochronology 10, 418–423. http://dx.doi.org/10.1016/j.quageo.2012.04.018.
Moreno, D., Falguères, C., Pérez-González, A., Voinchet, P., Ghaleb, B., Despriée, J., Bahain, J.-J., Sala, R., Carbonell, E., Bermúdez de Castro, J.M., Arsuaga, J.L., 2015. New radiometric dates on the lowest stratigraphical section (TD1 to TD6) of Gran Dolina site (Atapuerca, Spain). Quaternary Geochronology. http://dx.doi.org/10.1016/j.quageo.2015.05.007.
Navazo, M., 2006. Sociedades cazadoras-recolectoras en la Sierra de Atapuerca durante el Paleolítico medio: patrones de asentamiento y estrategias de movilidad. Universidad de Burgos, Burgos.
Navazo, M., Alonso-Alcalde, R., Benito-Calvo, A., Díez, J.C., Pérez-González, A., Carbonell, E., 2011. Hundidero: Mis 4 open air neanderthal occupations in sierra de atapuerca. Archaeology, Ethnology and Anthropology of Eurasia 39, 29–41. http://dx.doi.org/10.1016/j.aeae.2012.02.004.
Navazo, M., Carbonell, E., 2014. Neanderthal settlement patterns during MIS 4–3 in Sierra de Atapuerca (Burgos, Spain). Quaternary International 331, 267–277. http://dx.doi.org/10.1016/j.quaint.2014.03.032.
Ortega, A.I., Benito-Calvo, A., Pérez-González, A., Carbonell, E., Bermúdez de Castro, J.M., Arsuaga, J.L., 2014. Atapuerca Karst and its Palaeoanthropological Sites. In: Gutiérrez, F., Gutiérrez, M. (Eds.), Landscapes and Landforms of Spain, Word Geomorphological Landscapes. Springer, pp. 101–111.
Ortega, A.I., Benito-Calvo, A., Pérez-González, A., Martín Merino, M.A., Pérez-Martínez, R., Parés, J.M., Aramburu, A., Arsuaga, J.L., Bermúdez de Castro, J.M., Carbonell, E., 2013. Evolution of multilevel caves in the Sierra de Atapuerca (Burgos, Spain) and its relation to human occupation. Geomorphology 196, 122–137. http://dx.doi.org/10.1016/j.geomorph.2012.05.031.
Ortega, A.I., Benito-Calvo, A., Porres, J., Pérez-González, A., Martín Merino, M.A., 2010. Applying electrical resistivity tomography to the identification of endokarst geometries in the Pleistocene Sites of the Sierra de Atapuerca (Burgos, Spain). Archaeological Prospection 17, 233–245.
Ortega Martínez, A.I., 2009. La evolución geomorfológica del karst de la Sierra de Atapuerca (Burgos) y su relación con los yacimientos pleistocenos que contiene. Universidad de Burgos, Burgos.
Parés, J.M., Ortega, A.I., Benito-Calvo, A., Aranburu, A., Bermúdez de Castro, J.M., Carbonell, E., 2015. Paleomagnetic constraints on the Atapuerca Karst development (N Spain). In: Feinberg, J., Gao, Y., Calvin Alexandre, E. (Eds.), Caves and Karst across Time. GSA Special Volume.
Parés, J.M., Pérez-González, A., 1999. Paleomagnetic age for hominid fossils at Atapuerca Archaeological site, Spain. Science 269, 830–832.
Parés, J.M., Pérez-González, A., Arsuaga, J.L., Bermúdez De Castro, J.M., Carbonell, E., Ortega, A.I., 2010. Characterizing the sedimentary history of cave deposits, using archaeomagnetism and rock magnetism, Atapuerca (Northern Spain). Archaeometry 52, 882–898.
Parés, J.M., Pérez-González, A., Rosas, A., Benito, A., Bermúdez de Castro, J.M., Carbonell, E., Huguet, R., 2006. Matuyama-age lithic tools from the Sima del Elefante site, Atapuerca (northern Spain). Journal of Human Evolution 50, 163–169.
Pérez-González, A., Parés, J.M., Carbonell, E., Aleixandre, T., Ortega, A.I., Benito, A., Martín, M.A., 2001. Géologie de la Sierra de Atapuerca et stratigraphie des remplissages karstiques de Galería et Dolina (Burgos, Espagne). L'Anthropologie 105, 27–43. http://dx.doi.org/10.1016/S0003-5521(01)80004-2.
Pérez-González, A., Parés, J.M., Gallardo, J., Aleixandre, T., Ortega, A.I., Pinilla, A., 1999. Geología y estratigrafía del relleno de Galería de la Sierra de Atapuerca (Burgos). In: Carbonell, E., Rosas, A., Díez, J.C. (Eds.), Atapuerca: Ocupaciones Humanas Y Paleoecología Del Yacimiento de Galería. Junta de Castilla y León, Conserjería de Educación y Cultura, Valladolid, pp. 31–42.
Phillips, J.D., Lutz, J.D., 2008. Profile convexities in bedrock and alluvial streams. Geomorphology 102, 554–566. http://dx.doi.org/10.1016/j.geomorph.2008.05.042.
Pineda, A., Arce, J.M., 1997. Mapa Geológico de España, E 1:50.000, Hoja n° 200 (Burgos), Serie Magna. IGME, Madrid.
Rosas, A., Huguet, R., Pérez-González, A., Carbonell, E., Bermúdez de Castro, J.M., Vallverdú, J., van der Made, J., Allué, E., García, N., Martínez-Pérez, R., Rodríguez, J., Sala, R., Saladie, P., Benito, A., Martínez-Maza, C., Bastir, M., Sánchez, A., Parés, J.M., 2006. The "Sima del Elefante" cave site at Atapuerca (Spain). Estudios Geológicos 62, 327–348.

Schattner, M.L., 2010. Landscape evolution and hominin dispersal. Quaternary Science Reviews 29, 1495–1500.
Stanistreet, I.G., 2012. Fine resolution of early hominin time, Beds I and II, Olduvai Gorge, Tanzania. Journal of Human Evolution 63, 300–308.
Tsou, C.-Y., Chigira, M., Matsushi, Y., Chen, S.-C., 2014. Fluvial incision history that controlled the distribution of landslides in the Central Range of Taiwan. Geomorphology 226, 175–192. http://dx.doi.org/10.1016/j.geomorph.2014.08.015.
Wegmann, S.F.G., Franke, K.L., Hughes, S., Lewis, R.Q., Lyons, N., Paris, P., Ross, K., Bauer, J.B., Witt, A.C., 2011. Hillslope response to knickpoint migration in the Southern Appalachians: implications for the evolution of post-orogenic landscapes. Earth Surface Processes and Landforms 36, 1254–1267. http://dx.doi.org/10.1002/esp.2150.
Yenes, M., Monterrubio, S., Nespereira, J., Santos, G., Fernández-Macarro, B., 2015. Large landslides induced by fluvial incision in the Cenozoic Duero Basin (Spain). Geomorphology 246, 263–276. http://dx.doi.org/10.1016/j.geomorph.2015.06.022.
Zazo, C., Goy, J.L., Hoyos, M., 1983. Estudio geomorfológico de los alrededores de la Sierra de Atapuerca (Burgos). Estudios Geológicos 39, 179–185.